SIX DAYS THREE CONFERENCES THREE FORUMS ONE EXHIBITION

EuMW 2023
WAVES BEYOND WALLS

# EUROPEAN MICROWAVE WEEK

**Messe Berlin hub27**
**BERLIN, GERMANY**

**17th–22nd SEPTEMBER 2023**
**www.eumweek.com**

IN PERSON EVENT

26TH EDITION OF THE EUMW WEEK

# CONFERENCE PROGRAMME

EUROPE'S PREMIER MICROWAVE, RF, WIRELESS AND RADAR EVENT

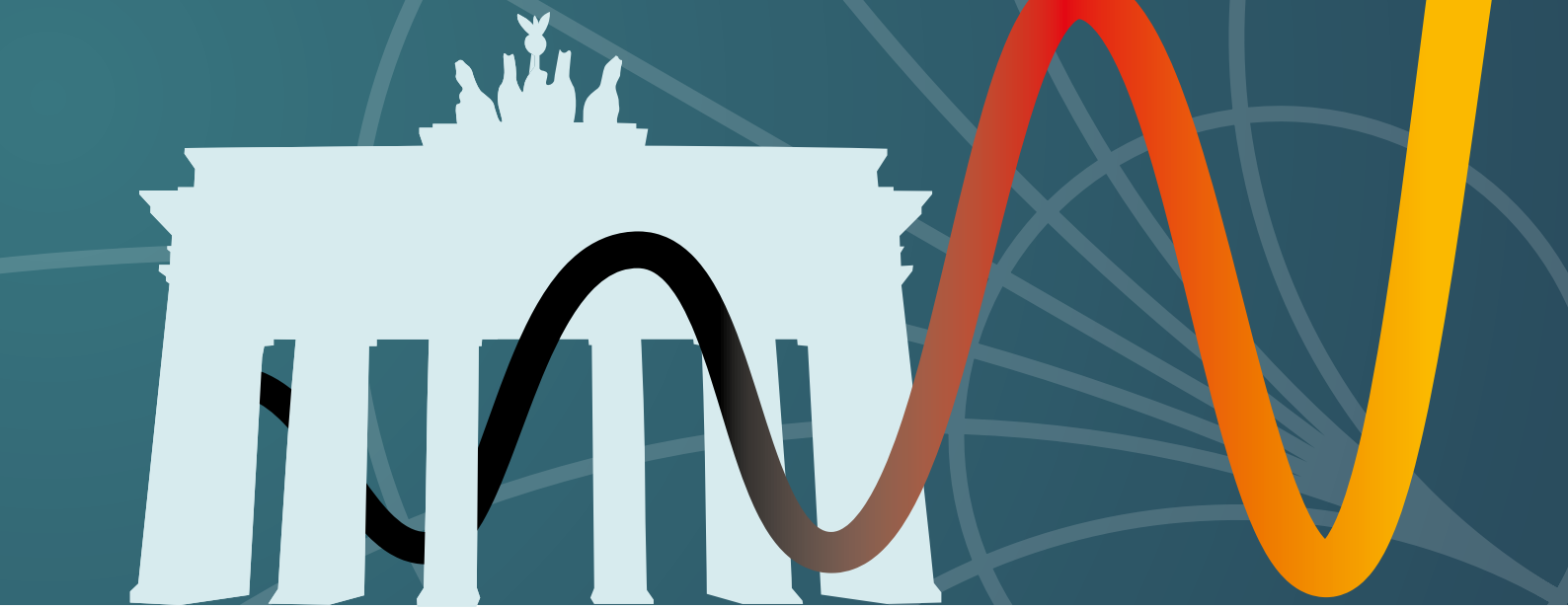

## WAVES BEYOND WALLS

Register online at: **www.eumweek.com**

53RD EUROPEAN MICROWAVE CONFERENCE 2023
The 53rd European Microwave Conference

EuMIC 2023
The 18th European Microwave Integrated Circuits Conference

EuRAD 2023
The 20th European Radar Conference

EuMA
European Microwave Association

horizon house

# TUESDAY 14:20 – 16:00

| ROOM | Beta 7 | Beta 8 | Beta 9 |
|---|---|---|---|
| | **EuMIC18**<br>PAs for Communication Systems<br>Chair: Rocco Giofrè[1]<br>Co-Chair: María J. Madero-Ayora[2]<br>[1]Università di Roma Tor Vergata, [2]Universidad de Sevilla | **EuMIC19**<br>Circuits for Broadband mm-Wave Transceivers<br>Chair: Hua Wang[1]<br>Co-Chair: Ulrich Lewark[2]<br>[1]ETH Zurich, [2]IMST GmbH | **EuMC06**<br>Multi-Functional and Reconfigurable Planar Filters<br>Chair: Christian Schulz[1]<br>Co-Chair: Vittorio Tornielli di Crestvolant[2]<br>[1]University of Alcala, [2]Ruhr-University Bochum |
| **14:20 – 14:40** | **EuMIC18-1**<br>Transmission Line Transformer Based Broadband Differential Class-E PA for Cellular Handset<br>Masatoshi Hase[1]<br>[1]Murata Manufacturing Co., Ltd. | **EuMIC19-1**<br>Design of an E-TSPC Flip-Flop for a 43 Gb/s PRBS Generator in 22 nm FDSOI<br>Florian Probst[1], Jonas Weninger[1], Andre Engelmann[1], Vadim Issakov[2], Robert Weigel[1]<br>[1]Friedrich-Alexander-Universität Erlangen-Nürnberg, [2]TU Braunschweig | **EuMC06-1**<br>Nonreciprocal Filtering Power Divider Using Mixed Static and Time-Modulated Resonators: Numerical Design Approach and Experimental Validation<br>Girdhari Chaudhary[1], Phanam Pech[1], Samdy Saron[1], Dimitra Psychogiou[2], Yongchae Jeong[1]<br>[1]Jeonbuk National University, South Korea, [2]University College Cork & Tyndall National Institute |
| **14:40 – 15:00** | **EuMIC18-2**<br>A 24 GHz Harmonic-Injection Doherty Power Amplifier with 42 % PAE at 6 dB OPBO in 100 nm GaN Technology<br>Moise Safari Mugisho[1], Christian Friesicke[1], Mohammed Ayad[2], Thomas Maier[1], Rüdiger Quay[1]<br>[1]Fraunhofer IAF, Fraunhofer Institute for Applied Solid State Physics, [2]UMS - United Monolithic Semiconductors | **EuMIC19-2**<br>A Silicon-Based Optical Signal Transmitter for Sub-THz Wireless Communication Systems<br>Kalliopi Spanidou[1], Luis Orbe[2], Robinson Cruzoe Guzmán[1], Luis González-Guerrero[1], Guillermo Carpintero[1]<br>[1]University Carlos III of Madrid, [2]Synopsys Photonics Solutions | **EuMC06-2**<br>Multi-Functional Bandpass Filters with Frequency Tunability and RF Co-designed Isolator Functionality<br>Kexin Li[1], Dimitra Psychogiou[1]<br>[1]UCC-Tyndall |
| **15:00 – 15:20** | **EuMIC18-3**<br>A Design Approach for Bandwidth Enhancement of 3-Way Doherty PAs<br>Anna Piacibello[1], Rocco Giofrè[2], Paolo Colantonio[2], Vittorio Camarchia[1]<br>[1]Politecnico di Torino, [2]Università di Roma "Tor Vergata" | **EuMIC19-3**<br>A 32 GHz, 12.8 GSps Direct Sampler and Converter for Direct Microwave Sampling for Terrestrial and Space Applications<br>Francois Bore[1]<br>[1]Teledyne E2V Semiconductors SAS | **EuMC06-3**<br>Ultrawide In-Band Self-Interference Suppression Using Bandpass Filter-Based RF Cancellers<br>Kevin Martin[1], Dimitra Psychogiou[1]<br>[1]University College Cork and Tyndall National Institute |
| **15:20 – 15:40** | **EuMIC18-4**<br>A 20-Watts, GaN MMIC Doherty Power Amplifier for Ku-Band Satellite Communications<br>Seifeddine Fakhfakh[1]<br>[1]United Monolithic Semiconductors (UMS) | **EuMIC19-4**<br>A Fully-Differential Travelling-Wave Amplifier up to 110 GHz in a 22 nm FD-SOI CMOS Technology<br>Athanasios Gatzastras[1], Christian Volmer[2], Ingmar Kallfass[3]<br>[1]Institute of Robust Power Semiconductor Systems (ILH) - University of Stuttgart, [2]Advantest Europe GmbH, [3]Institute of Robust Power Semiconductor Systems (ILH), University of Stuttgart, Stuttgart, Germany | **EuMC06-4**<br>Non-Reciprocal RF Co-Designed Filtering Phase Shifters With Continuously Tunable Phase Shift<br>Zixiao Zhang[1], Dimitra Psychogiou[1]<br>[1]UCC-Tyndall |
| **15:40 – 16:00** | **EuMIC18-5**<br>A 39.5 dBm GaN Doherty Amplifier MMIC with Phase Control for Ka-band Space Applications<br>Jose Romero Lopera[1], Michael Ernst Gadringer[1], Erich Leitgeb[1], Wolfgang Bösch[1], Helmut Paulitsch[1]<br>[1]Graz University of Technology | **EuMIC19-5**<br>A D-band Low-Noise Amplifier in 28-nm CMOS Technology for Radio Astronomy Applications<br>Li-Jung Huang[1], Chau-Ching Chiong[2], Yunshan Wang[1], Huei Wang[1], Chung-Chia Chien[1]<br>[1]National Taiwan University, [2]Institute of Astronomy and Astrophysics, Academia Sinica | **EuMC06-5**<br>Signal-Interference Bandpass Filters Using Resonant Transversal Filtering Sections With Asymmetrical Transfer Function Characteristics<br>David Chatzichristodoulou[1], Symeon Nikolaou[2], Photos Vryonides[2], Dimitra Psychogiou[3]<br>[1]Frederick Research Center, Cyprus , [2]Frederick Research Center, Cyprus, [3]Tyndall National Institute, Cork, T12 R5CP, Ireland |

# Nonreciprocal Filtering Power Divider Using Mixed Static and Time-Modulated Resonators: Numerical Design Approach and Experimental Validation

Girdhari Chaudhary[#], Phanam Pech[#], Samdy Saron[#], Dimitra Psychogiou[*^], Yongchae Jeong[#]

[#]Jeonbuk National University, South Korea

[*]University College Cork, Ireland

[^]Tyndall National Institute, Ireland

girdharic@jbnu.ac.kr, ycjeong@jbnu.ac.kr

***Abstract* — This paper presents detailed design methodology and the experimental validation of a nonreciprocal power divider ($|S_{21}| \neq |S_{12}|$ and $|S_{31}| \neq |S_{13}|$) using mixed static and time-modulated resonators. The nonreciprocal response is achieved by modulating its constituent resonators with a sinusoidal signal with progressive phase shift. The mixed static and time-modulated resonators are used to achieve a wider bandwidth for the reverse isolation ($|S_{12}|$ and $|S_{13}|$) while using fewer time-modulated resonators. The analytical spectral *S*-parameters of the nonreciprocal power divider have been derived to simplify the design method. General empirical design equations for the modulation parameters are derived from numerical simulations, which enable the proposed nonreciprocal power divider with the desired specifications. For experimental validation, a nonreciprocal filtering power divider with an equal power division ratio was designed and fabricated at center frequency of 1.45 GHz. The measured results confirmed the accuracy of the analytical design equations.**

***Keywords* — Analytical spectral S-parameters, mixed static and time-modulated resonators, nonreciprocal filtering power divider, varactor diode.**

## I. Introduction

Next generation wireless communication systems demand a cost effective and multi-functional circuits to reduce the size of the RF front-end. As example of this trend is the RF filtering power divider that combines the function of filter and a power divider within the volume of a single RF component. However, conventional power dividers are reciprocal ($|S_{21}| = |S_{12}|$ and $|S_{31}| = |S_{13}|$) in nature [1]. Therefore, integrating the filtering power divider and isolator in a single circuit has been attracting significant interest for the next generation communication systems. Traditionally, nonreciprocal circuits such as isolators and circulators are designed using magnetic material such as ferrites, which are bulky and expensive [2].

In recent years, there has been a growing interest in the design of a nonreciprocal bandpass filter (NBPF) using time-modulated resonators that avoid the need of magnetic materials and allow transmission in single direction [3]-[7]. To achieve satisfactory forward insertion loss (IL), return loss (RL), and backward isolation (IX) with two nulls, most of the existing design concept use at least three time-modulated resonators with a progressive phase shift, which increases circuit complexity of modulation signal network [3]-[6]. A recently proposed nonreciprocal filtering power divider [8] requires six time-modulated resonators, which further increases the complexity of modulation signal circuit. Additionally, no analytical spectral *S*-parameters are derived to simplify the design method.

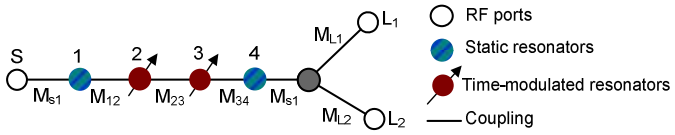


Fig. 1. Coupling diagram of proposed nonreciprocal filtering power divider.

In this paper, we present a design of a nonreciprocal filtering power divider that combines filtering power divider and isolator functions into a single circuit, thereby reducing the number of required components. The static resonators are coupled with time-modulated resonators to create two nulls in the reverse isolation direction and decrease the number of the time-modulated resonators. To simplify design, analytical spectral *S*-parameters are derived and are presented in the next section.

## II. Design Theory

### A. Spectral S-parameters of Nonreciprocal Power Divider

Fig. 1 shows the coupling diagram of the proposed nonreciprocal filtering power divider, which consists of mixed static and time-modulators resonators. Resonators 2 and 3 are modulated with a sinusoidal signal with a progressive phase shift. To achieve a nonreciprocal response, the capacitor of resonator is modulated with a progressive phase shift sinusoidal [3] as follows:

$$C(t) = C_0\left[1 + m\cos\{\omega_m t + \varphi_i\}\right],\ \varphi_i = (i-1)\Delta\varphi, \qquad (1)$$

where $\omega_m$, $\Delta\varphi$, and $m$ are modulation frequency, phase shift, and the modulation index, respectively. Likewise, $C_0$ is the nominal capacitance. The phase difference is the key mechanism that enables nonreciprocal response.

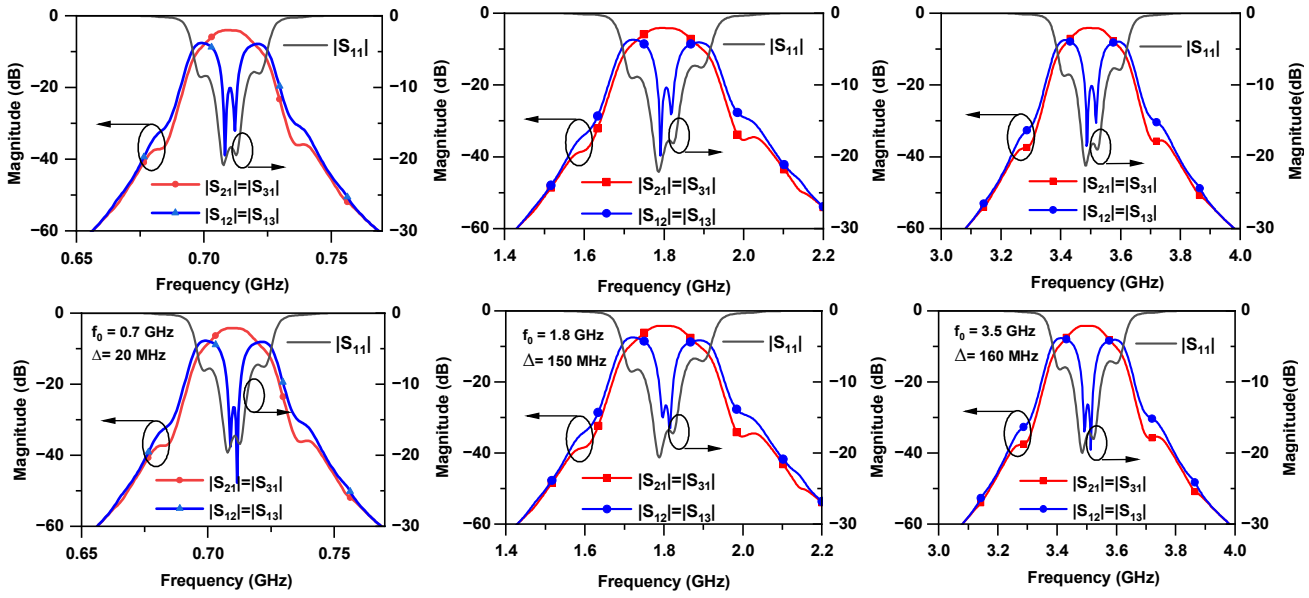


Fig. 2. Numerical simulation results of the proposed nonreciprocal filtering power divider: (a) $f_0$ = 0.71 GHz, Δ = 20 MHz, (b) $f_0$ = 1.8 GHz, Δ = 150 MHz, and (c) $f_0$ = 3.5 GHz, Δ = 150 MHz.

Table 1. Parameters of proposed nonreciprocal power divider

| $M_{S1}$ = 1.0352, $M_{12}$ = $M_{34}$=0.9106, $M_{23}$=0.6999, $M_{L1}$ = $M_{L2}$ = 0.7071 | | | | | | |
|---|---|---|---|---|---|---|
| $f_0$ (GHz) | 0.71 | | 1.80 | | 3.50 | |
| Δ (MHz) | 20 | | 150 | | 160 | |
| $f_m$ (MHz) | 15.6 | | 117 | | 124.8 | |
| Δφ (Deg) | 70° | | | | | |
| $m$ | 0.038 | 0.04 | 0.1125 | 0.1183 | 0.0617 | 0.0649 |
| IL (dB) | 1.06 | 1.19 | 1.04 | 1.17 | 1.06 | 1.18 |
| IX (dB) | 20.25 | 26.46 | 20.68 | 26.69 | 20.22 | 26.28 |
| RL (dB) | 18.3 | 17.26 | 17.8 | 16.94 | 18.16 | 17.14 |

IL: Insertion loss of forward transmission ($|S_{21}|$= $|S_{31}|$) at $f_0$ excluding 3.01 dB power division. IX: Reverse isolation ($|S_{12}|$ =| $S_{13}|$) at $f_0$

Using a ($N$+2) coupling matrix, the spectral $S$-parameters of the proposed nonreciprocal filtering power divider are derived in (2).

$$\mathbf{S}_{11} = U - \frac{2\mathbf{Q}\left(\mathbf{M}_{23}^2\lambda_1 + \mathbf{M}_{12}^2\lambda_3\right) + j\mathbf{A}-\mathbf{B}}{\mathbf{Q}\left(\mathbf{M}_{12}^2\lambda_3 + \mathbf{M}_{23}^2\lambda_1\right) - j\mathbf{M}_{23}^2\mathbf{Q}^2 + j\lambda_2\lambda_3\mathbf{Q}^2 + j\mathbf{C} + \mathbf{D}} \tag{2a}$$

$$\mathbf{S}_{21} = \mathbf{S}_{31} = \frac{2\mathbf{Q}\mathbf{M}_{12}^2\mathbf{M}_{23}\mathbf{M}_{L1}}{\mathbf{Q}\left(\mathbf{M}_{12}^2\lambda_3 + \mathbf{M}_{23}^2\lambda_1\right) - j\mathbf{M}_{23}^2\mathbf{Q}^2 + j\lambda_2\lambda_3\mathbf{Q}^2 + j\mathbf{C} + \mathbf{D}} \tag{2b}$$

$$\mathbf{S}_{12} = \mathbf{S}_{13} = \frac{2\mathbf{Q}\mathbf{M}_{12}^2\mathbf{M}_{23}\mathbf{M}_{L1}}{\mathbf{Q}\left(\mathbf{M}_{12}^2\lambda_3 + \mathbf{M}_{23}^2\lambda_1\right) - j\mathbf{M}_{23}^2\mathbf{Q}^2 + j\lambda_3\lambda_2\mathbf{Q}^2 + j\mathbf{C}_1 + \mathbf{D}_1} \tag{2c}$$

where

$$\mathbf{A} = 4\mathbf{M}_{L1}^2\left(\mathbf{M}_{12}^2\lambda_1\lambda_2 + \mathbf{M}_{12}^2\lambda_3\lambda_4 + \mathbf{M}_{23}^2\lambda_1\lambda_4 - \mathbf{M}_{12}^4\right) \tag{3a}$$

$$\mathbf{B} = 2\lambda_1\lambda_2\lambda_3\mathbf{M}_{s1}^2 + j4\mathbf{M}_{L1}^2\lambda_1\lambda_2\lambda_3\lambda_4 \tag{3b}$$

$$\mathbf{C} = 2\mathbf{M}_{L1}^2\left(\mathbf{M}_{12}^2\lambda_1\lambda_2 - \mathbf{M}_{12}^4 + \mathbf{M}_{12}^2\lambda_3\lambda_4 + \mathbf{M}_{23}^2\lambda_1\lambda_4 - \lambda_1\lambda_2\lambda_3\lambda_4\right) \tag{3c}$$

$$\mathbf{D} = 2\mathbf{Q}\mathbf{M}_{L1}^2\left(\mathbf{M}_{12}^2\lambda_2 + \mathbf{M}_{23}^2\lambda_4\right) - \mathbf{Q}\left(\lambda_1\lambda_2\lambda_3 + 2\mathbf{M}_{L1}^2\lambda_2\lambda_3\lambda_4\right) \tag{3d}$$

$$\mathbf{C}_1 = 2\mathbf{M}_{L1}^2\left(\mathbf{M}_{12}^2\lambda_2\lambda_1 - \mathbf{M}_{12}^4 + \mathbf{M}_{12}^2\lambda_4\lambda_3 + \mathbf{M}_{23}^2\lambda_4\lambda_1 - \lambda_4\lambda_3\lambda_2\lambda_1\right) \tag{3e}$$

$$\mathbf{D}_1 = 2\mathbf{Q}\mathbf{M}_{L1}^2\left(\mathbf{M}_{12}^2\lambda_2 + \mathbf{M}_{23}^2\lambda_4\right) - \mathbf{Q}\left(\lambda_3\lambda_2\lambda_1 + 2\mathbf{M}_{L1}^2\lambda_4\lambda_3\lambda_2\right) \tag{3f}$$

The coupling matrix values are defined as: $\mathbf{Q} = M_{S1}U$, $\mathbf{M_{12}} = M_{12}U = M_{34}U$, $\mathbf{M_{23}} = M_{23}U$, $\mathbf{M_{L1}} = M_{L1}U = M_{L2}U$. Similarly, $U$ is an identity matrix. It should be noted that each resonator generates a number of nonlinear harmonics, which are coupled by time-modulated capacitors. For simplicity, we consider only two nonlinear harmonics, and the spectral admittance matrix of time-modulated resonator is given in (4).

$$\lambda_i = \begin{bmatrix} \Omega_{-2} & \frac{x_{-2}m}{2\omega_0\Delta}e^{-j\varphi_i} & 0 & 0 & 0 \\ \frac{x_{-1}m}{2\omega_0\Delta}e^{j\varphi_i} & \Omega_{-1} & \frac{x_{-1}m}{2\omega_0\Delta}e^{-j\varphi_i} & 0 & 0 \\ 0 & \frac{x_0m}{2\omega_0\Delta}e^{j\varphi_i} & \Omega_0 & \frac{x_0m}{2\omega_0\Delta}e^{-j\varphi_i} & 0 \\ 0 & 0 & \frac{x_1m}{2\omega_0\Delta}e^{-j\varphi_i} & \Omega_{+1} & 0 \\ 0 & 0 & 0 & \frac{x_{+2}m}{2\omega_0\Delta}e^{j\varphi_i} & \Omega_{+2} \end{bmatrix}, \tag{4}$$

where

$$\Omega_n = \frac{\omega_0}{\Delta}\left(\frac{x_n}{\omega_0} - \frac{\omega_0}{x_n}\right), \tag{5a}$$

$$x_n = \omega + n\omega_m,\ n = -2,-1,0,1,2 \tag{5b}$$

Similarly Δ and $\omega_0$ are the bandwidth and the center angular frequency of filtering power divider. As seen from (2), it should be noted that spectral $S$-parameters are generated with an order equal to the order of harmonics components to achieve nonreciprocal response. The nonreciprocal response is achieved due to the difference between (2b) and (2c), which is owed to the generation of intermodulation (IM) products resulting from the modulation of resonators with a progressive phase shift sinusoidal signal.

For equal power division ratio, the values of $M_{L1}$ and $M_{L2}$ are given in (6).

$$M_{L1} = M_{L2} = \frac{1}{\sqrt{2}} \tag{6}$$

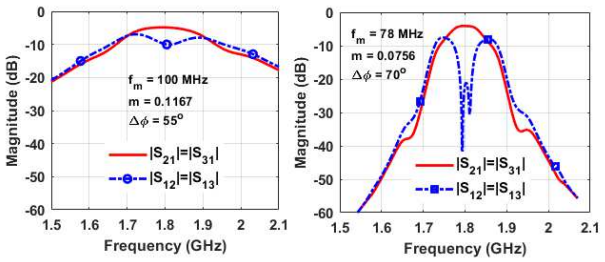


(a) (b)

Fig. 3. Numerical simulation results of nonreciprocal filtering power divider: (a) without static resonators and (b) with static resonators.

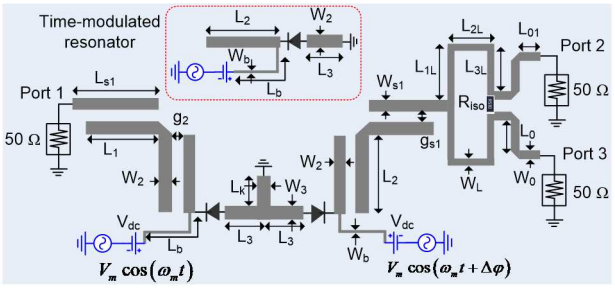


Fig. 4 Microstrip line implementation of the proposed nonreciprocal power divider. Physical dimensions: $W_0$ = 2.40, $W_{s1}$ = 1.34, $W_2$ = 2.5, $W_3$ = 2.27, $g_{s1}$ = 0.2, $g_2$ = 0.56, $L_{s1}$ = 47, $L_1$ = 44, $L_2$ = 29.4, $L_3$ = 11.2, $L_k$ = 1.94, $L_{1L}$ = 20.2, $L_{2L}$ = 6.3, $L_{3L}$ = 17.4, $L_0$ = 10, $L_{01}$ = 2, $W_b$ = 1, $L_b$ = 22. Unit: millimeter (mm). Varactor: SMV1233-079LF from Skyworks and $R_{iso}$ = 100 Ω.

Similarly, the remaining coupling matrix values ($M_{S1}$, $M_{12}$, $M_{23}$ and $M_{34}$) can be synthesized with Chebyshev equiripple or Butterworth response. To improve the isolation ($|S_{23}|$) between the output ports, a 100 Ω resistor needs to be connected.

### *B. Numerical Simulation Results and Discussion*

The analytical design equations derived in the previous sections can be directly used to compute the nonreciprocal response of the proposed power divider. It should be noted that only resonators 2 and 3 are modulated, while resonators 1 and 4 are static and no modulation is signal applied to them. The static resonators are used to achieve two nulls in reverse isolation without increasing the number of modulated resonators.

Numerical simulations have been carried out using the equations for different center frequency and bandwidth, and the results are shown in Figs. 2 and 3. The coupling matrix values are synthesized using the Chebyshev response with an equiripple of 0.043 dB. Table 1 summarizes the numerical simulation results. As observed from these figures, the proposed power divider provides a nonreciprocal response with two nulls in the reverse isolation. These numerical simulation results reveal IL < 1.2 dB, RL > 17 dB, and IX ($|S_{12}|$=$|S_{13}|$) < 20.2 dB and < 26.5 dB within the passband.

Based on these numerical simulation results, an interesting relationship among the modulation parameters ($f_m$, $m$, and $\Delta\varphi$), $f_0$, and $\Delta$ of the proposed nonreciprocal power divider can be set out empirically as (7).

$$f_m = 0.78\times\Delta,\quad m = \frac{1.35\times\Delta}{f_0},\quad 65^o \le \Delta\varphi \le 70^o \qquad (7)$$

It should be noted that (7) provides design relationships for achieving a reverse isolation of 20 dB at the center frequency by defining $f_0$ and $\Delta$ of the proposed filtering power divider. The modulation frequency is proportional to $\Delta$ of the nonreciprocal filtering power divider, whereas the modulation index depends on $f_0$ and $\Delta$. Furthermore, these empirical relations given in (7) provides an optimization-free design method of the proposed nonreciprocal filtering power divider.

Fig. 3 shows the simulation results of the nonreciprocal filtering power divider with and without static resonators. Two distinct nulls in IX are observed for the case of mixed static and time-modulated resonators, providing wideband and high reverse isolation without increasing the number of modulation signals.

## III. Experimental Results

To experimentally validate the proposed structure, a nonreciprocal filtering power divider was designed and fabricated on a Taconic substrate with a dielectric constant of 2.2 and a thickness of 0.787 mm, at center frequency of $f_0$ = 1.46 GHz and an equiripple bandwidth of $\Delta$ = 160 MHz. The goal was to achieve IX > 20 dB at $f_0$. As described in previous section, the modulation parameters of nonreciprocal filter are estimated using (7) as $f_m$ = 124.8 MHz, $m$ = 0.1479, and $\Delta\varphi$ = 70°.

Fig. 4 shows the microstrip line implementation of the proposed nonreciprocal power divider. The time-modulated resonators 2 and 3 are implemented using transmission line (TL) loaded with varactor, whereas static resonators are implemented with half-wavelength TL [6]. The coupling between time-modulated resonators 2 and 3 is realized through short-circuited shunt stub with physical parameter $W_3$ and $L_k$. Similarly, coupling between static and time-modulated resonators (1 and 2, 3 and 4) are implemented by controlling the physical parameter $W_2$, $L_2$, and $g_2$. Likewise, the coupling between the input RF ports, and resonators 1 and 4 are controlled through the physical parameters $L_{s1}$, $W_{s1}$, and $g_{s1}$. The time-varying capacitors are implemented by the modulating varactor SMV-1233-079LF from Skyworks Inc. In this work, modulation signal is applied to time-varying resonators through TL with physical parameters $W_b$ and $L_b$ for simplifying the modulation circuit. The simulation was performed using ANSYS high frequency structure simulator (HFSS) and PathWave Advanced Design System (ADS) in conjunction with a large signal scattering analysis module. The physical dimensions of the fabricated circuit are shown in Fig. 4.

Figs. 5 and 6 show the EM simulation and the RF measured results of the nonreciprocal filtering power divider. The modulation parameters of $f_m$ = 125 MHz, $\Delta\varphi$ = 70°, and $V_m$ = 1.2 V are applied to achieve nonreciprocal response. The measurement results are well agreed with simulations. At $f_0$ of 1.45 GHz, the measured forward transmission magnitudes are $|S_{21}|$ = -5.93 dB and $|S_{31}|$ = -5.96 dB, with a forward transmission 3-dB bandwidth of 150 MHz. The measured IX at $f_0$ are $|S_{12}|$ = -28.77 dB and $|S_{13}|$ = -29.05 dB and 18 dB

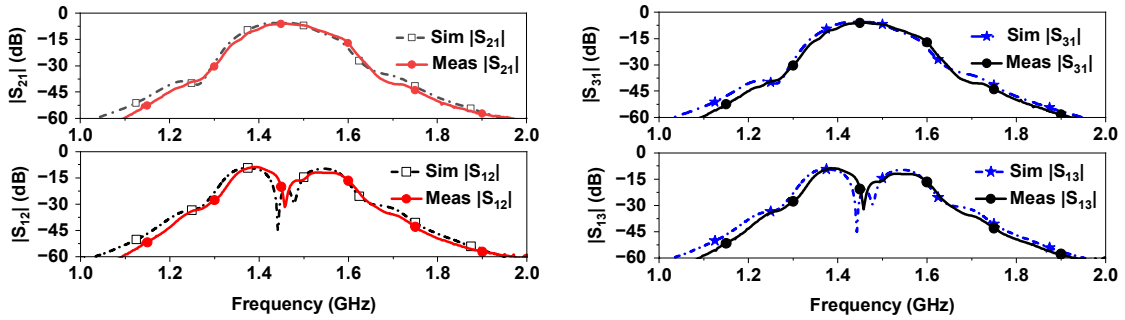


(a)

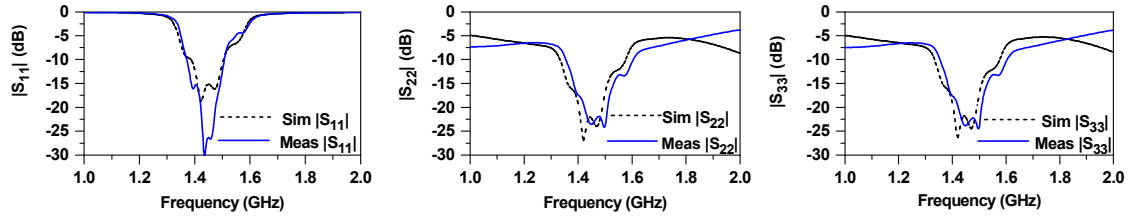


(b)

Fig. 5. EM simulated and RF measured *S*-parameters of the nonreciprocal filtering power divider: (a) forward transmission/reverse isolation and (b) return losses.

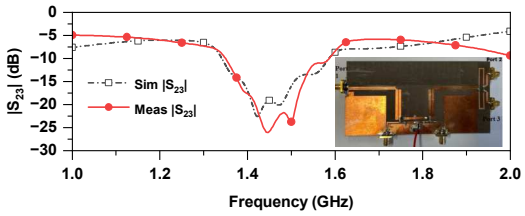


Fig. 6. EM simulated and RF measured isolation between the output ports.

Table 2. Comparison between proposed work with state of arts

| | $f_0$ (GHz) | NTR | IL (dB) | IX@$f_0$ (dB) | IX nulls |
|---|---|---|---|---|---|
| [3] | 0.19 | 3* | 1.50 | 20.2 | 2 |
| [4] | 0.143 | 3* | 3.70 | 34.8 | 1 |
| [8] | 2.40 | 6** | 3.92 | 27.82 | 1 |
| **This work** | **1.46** | **2** | **2.94** | **28.77** | **2** |

NTR: number of time-modulated resonators, *: NBPF, **: nonreciprocal power divider, IL: insertion loss excluding 3.01 dB power division.

reverse isolation bandwidth is 40 MHz, shaped by two distinct isolation nulls.

The input and output return loss are better than 20 dB at $f_0$. The isolation between output ports is higher than 20 dB at 1.46 GHz. The photograph of manufactured circuit is shown in Fig. 6. Table 2 shows the performance comparison of the proposed nonreciprocal filtering divider with the state-of-arts. As seen from table 2, the proposed nonreciprocal power divider provides high and wider bandwidth IX having two nulls with a fewer number of time-modulated resonators.

## IV. Conclusion

In this paper, we demonstrated a nonreciprocal filtering power divider using static and time-modulated resonators. By coupling static resonators with time-modulated resonators, two nulls in the reverse isolation are created, which allows for a reduction in the number of time-modulated resonators and simplifies the modulation signal circuit. Analytical spectral *S*-parameters are derived in this work, which facilitates the determination of optimum modulation parameters easily.


## Acknowledgment

This research was supported by National Research Foundation of Korea (NRF) grant funded by Korea Government (Ministry of Science and ICT: MSIT) (No. RS-2023-00209081) and in part by the Basic Science Research Program through the NRF grant funded by Ministry of Education (No. 2019R1A6A1A09031717).


## References


[1] P. Kim, G. Chaudhary, and Y. Jeong, "Analysis and design of an unequal termination impedance power divider with bandpass filtering response," *IET Electronics Letters*, vol. 53, no. 18, pp 1260-1262, Aug. 2017.

[2] C. E. Fay and R. L. Comstock, "Operation of the ferrite junction circulator," *IEEE Trans. Microw. Theory Techn.*, vol. MTT-13, no. 1, pp. 15–27, Jan. 1965.

[3] X. Wu, X. Liu, M. D. Hickle, D. Peroulis, J. S. Gomez-Dıaz, and A. Alvarez Melcon, "Isolating bandpass filters using time-modulated resonators," *IEEE Trans. Microw. Theory Techn.*, vol. 67, no. 6, pp 2331–2345, Jun. 2019.

[4] D. Simpson and D. Psychogiou, "Magnet-less non-reciprocal bandpass filters with tunable center frequency," *in Proc. Eur. Microw. Conf*, pp. 460–463, Oct. 2019.

[5] G. Chaudhary and Y. Jeong, "Frequency tunable impedance matching nonreciprocal bandpass filter using time-modulated quarter-wave resonators," *IEEE Trans. Industrial Electronics*, vol. 69, no. 8, pp. 8356-8365, Aug. 2022.

[6] G. Chaudhary and Y. Jeong, "Nonreciprocal bandpass filter using mixed static and time-modulated resonators," *IEEE Microw. Wireless Compon. Letters*, vol. 32, no. 4, pp. 297-300, Apr. 2022.

[7] G. Chaudhary, J. Lee, P. Pech, and Y. Jeong, "Microstrip line non-reciprocal bandpass filter with tunable center frequency," *Proc. IEEE International Sympo. Radio-Frequency Integration Tech. (RFIT),* pp. 188-190, Aug. 2022.

[8] J. Zang, S. Wang, A. Alvarez-Melcon, J. S. Gomez Diaz, "Nonreciprocal filtering power dividers," *Int. J. Electron. Commun.* (AEU), 132, 153609, 2021.